Title

ESTIMATES OF RADIOACTIVE DECAY BY THE EMISSION OF NUCLEI HEAVIER THAN ALPHA PARTICLES

Authors

Shi, Y-J.
Swiatecki, W.J.

Publication Date

1984-09-01

LBL-18349
Preprint

Lawrence Berkeley Laboratory
UNIVERSITY OF CALIFORNIA

Submitted to Nuclear Physics

ESTIMATES OF RADIOACTIVE DECAY BY THE EMISSION OF NUCLEI HEAVIER THAN ALPHA PARTICLES

Y-J. Shi and W.J. Swiatecki

September 1984

Prepared for the U.S. Department of Energy under Contract DE-AC03-76SF00098

DISCLAIMER

LBL-18349

Estimates of Radioactive Decay by the Emission of Nuclei Heavier than Alpha Particles

Shi Yi-Jin*

and

W. J. Swiatecki

Nuclear Science Division
Lawrence Berkeley Laboratory
University of California
Berkeley, California 94720

September, 1984

This work was supported by the Director, Office of Energy Research, Division of Nuclear Physics of the Office of High Energy and Nuclear Physics of the U.S. Department of Energy under Contract DE-AC03-76SF00098.

*Permanent address: Institute of Atomic Energy, P. O. Box 275 (18), Beijing, China

LBL-18349

Estimates of Radioactive Decay by the Emission of Nuclei Heavier than Alpha Particles

Shi Yi-Jin*

and

W. J. Swiatecki

Nuclear Science Division
Lawrence Berkeley Laboratory
University of California
Berkeley, California 94720

Abstract

We estimate the lifetimes for radioactive decay of a nucleus by the emission of alpha paticles or heavier fragments like ^{14}C, by treating these processes as extreme cases of spontaneous fission. The lifetime is accordingly written as a frequency factor of the order of collective nuclear oscillations (10^{-21} - 10^{-22}sec) times a Gamow penetrability factor for the appropriate deformation-energy barrier. For the very asymmetric decays, an approximation to the barrier is obtained by combining the Coulomb repulsion between the fragments with the nuclear proximity potential (up to contact) and interpolating smoothly between the contact configuration and the configuration of the parent nucleus. We give a closed formula for the penetrability factor and find that to within about one power of ten, we can account for the recently observed branching ratios between alpha particle and ^{14}C emissions from $^{222,223,224}Ra$. We apply our method to calculate branching ratios for other exotic decays (involving isotopes of O, Ne among others) and estimate that there may be a number of such decays that will be accessible to observation.

This work was supported by the Director, Office of Energy Research, Division of Nuclear Physics of the Office of High Energy and Nuclear Physics of the U.S. Department of Energy under Contract DE-AC03-76SF00098.

*Permanent address: Institute of Atomic Energy, P. O. Box 275 (18), Beijing, China

1. Introduction

The recently discovered (ref. 1) spontaneous radioactive decay of ^{223}Ra into Pb^{209} by the emission of ^{14}C has been confirmed in refs. 2,3, and similar decays of ^{222}Ra into ^{208}Pb and of ^{224}Ra into ^{210}Pb have been reported in ref. 3. The ratios of the rates of these exotic decay modes to the corresponding rates of α-particle emission are given in ref. 3 as $(3.7 \pm 0.5) \times 10^{-10}$, $(6.1 \pm 0.8) \times 10^{-10}$ and $(4.3 \pm 1.1) \times 10^{-11}$ for ^{222}Ra, ^{223}Ra and ^{224}Ra, respectively. In refs. 1,3 These experimental branching ratios have been compared only with the ratios of Gamow penetrability factors for pure Coulomb barriers, cut off at a sharp (contact) distance, parameterized as $r_o (A_1^{1/3} + A_2^{1/3})$, where A_1, A_2 are the mass numbers of the two decay fragments. Values of r_o in the range of 1.15–1.25 fm were tried in ref. 1 with the result that the Gamow factors would, by themselves, lead to branching ratios several orders of magnitude higher than the observed values. In ref. 1 the conclusion is drawn that, in the case of ^{223}Ra, the emission rate of ^{14}C may be understood as a barrier penetration phenomenon slowed down by a "preformation probability factor" in the range of 7×10^{-5} – 4×10^{-7} times the preformation probability for α-emission from the same nucleus.

In this paper, we would like to draw attention to the fact that if a more realistic estimate of the potential-energy barrier is used in the penetrability calculation, the branching ratios come out to be reasonably close to the three measured values (without the use of any adjustable parameters and without invoking hypothetical preformation probability factors). This appears to us consistent with the point of view that the emission of fragments like ^{14}C—and even, to a certain extent, α-emission—

may be looked upon simply as extremely asymmetric types of spontaneous fission (ref. 8). In such an approach one expects to be able to estimate the decay lifetime as the product of a frequency factor of the order of nuclear collective oscillations (in the range 10^{-22}–10^{-21} sec) times a penetrability factor through a properly estimated deformation-energy barrier. There is no room in such fission-like calculations for preformation factors of several powers of ten. Thus, in the case of Uranium fission, for example, one does not have to wait for a Barium fragment, say, to be preformed inside the parent nucleus. The Barium is not "preformed," but takes shape as part of the geometrical deformation process, i.e., as part of the process of barrier penetration itself.

2. The Barrier Penetrability Calculation

To implement this point of view, we have constructed deformation-energy barriers by modifying the Coulomb repulsion between the fragments by the nuclear Proximity potential up to contact of the fragments, and continuing beyond contact by an interpolation to the configuration of the parent nucleus. Fig. 1 shows such barriers for the decay of ^{222}Ra by α and by ^{14}C emission. (See also Fig. 2.) The abscissa is in fermis and gives the major axis L (i.e. the extreme extension) of the configuration in question (upper scale) or the distance z between the near surfaces of the fragments (lower scale). The value $L = L_c = 2\ (C_1 + C_2) = 2r_c$ corresponds to contact of the fragments, assumed spherical and with radii C_1 and C_2 (r_c is the center separation at contact). Down to contact the potential was calculated using the canonical Proximity potential of refs. 4,5 without the adjustment of any parameters. After contact, when the two fragments are

fusing, the proximity treatment soon becomes inapplicable. To estimate the appearance of the deformation energy below contact, we had recourse to a smooth power-law interpolation between $L = 2r_c$ and $L = L_o = 2C$, where C corresponds to the radius of the compound system (the parent nucleus). (For this value of L the deformation potential is zero by definition). This is a somewhat arbitrary prescription for interpolating the deformation energy between V(contact) and V = 0 but, as seen from Fig. 1, only a relatively small part of the potential-energy barrier is affected by this uncertainty. The major part of the barrier, even in the case of ^{14}C emission, corresponds to configurations of separated fragments. This makes an estimate of the deformation energy for these very asymmetric divisions far easier and more reliable than for conventional fission processes.

The explicit expression for the deformation energy V(L) is

$$V(L) = M_1 + M_2 - M + \frac{Z_1 Z_2 e^2}{r} + V_p(z) \qquad \text{for } L > L_c \tag{1}$$

$$V(L) = a\,(L - L_o)^{\nu} \qquad \text{for } L_o < L < L_c, \tag{2}$$

where $r = L - C_1 - C_2$ is the separation between fragment centers and a and ν are parameters determined by the requirement of a smooth fit at $L = L_c$. In the above, M_1, M_2 are the masses (or mass defects) in MeV and Z_1, Z_2 the atomic numbers of the two fragments, $e^2 = 1.4400$ MeV fm, and $V_p(z)$ is the nuclear proximity interaction given by

$$V_p(z) = K\Phi(z/b) \quad , \tag{3}$$

where $K = 4\pi\bar{R}\gamma b$, $\bar{R}$ is the reduced radius of the system, given by $C_1C_2/(C_1 + C_2)$, γ is the nuclear surface tension coefficient, b is the width (diffuseness) of the nuclear surface and Φ is the universal nuclear proximity function. We have used the following formulae from refs. 4,5:

$$\gamma = 0.9517\ [1 - 1.7826\ (\frac{N-Z}{A})^2]\text{MeV/fm}^2 \quad , \tag{4}$$

where N,Z,A refer to the neutron, proton and mass numbers of the parent nucleus, b = 1 fm, and the ("central") radius C_i (C_1,C_2 or C) is given in terms of the effective sharp radius R_i by

$$C_i = R_i - \frac{b^2}{R_i} \quad , \tag{5}$$

where a semi-empirical formula for R_i is given in ref. 4 as

$$R_i = 1.28\ A_i^{1/3} - 0.76 + 0.8\ A_i^{-1/3}\text{fm} \quad . \tag{6}$$

The Gamow penetrability factor G is given by

$$G = e^{\frac{2}{\hbar}\int_{z_o}^{z_{exit}} \sqrt{2M_r V}\, dz}$$

$$= e^{2\sqrt{2A_r}\,\frac{mc^2}{\hbar c}\int_{z_o}^{z_{exit}} \sqrt{V}\, dz}$$

$$= e^{(0.43749/\sqrt{\text{MeV}})(b/\text{fm})\sqrt{A_r}\ S} \quad , \tag{7}$$

where M_r is the effective mass appropriate to the disintegration degree of

freedom, and which we take to be simply the reduced mass of the separating fragments, since most of the barrier penetration is taking place in the post-scission regime. The reduced mass number, A_1A_2/A, is denoted by A_r and mc^2 is the nuclear mass unit, which we took as 931.5 MeV. The penetrability integral S is given by

$$S = \int_{\zeta_o}^{\zeta_{exit}} \sqrt{V(\zeta)}\, d\zeta \quad , \tag{8}$$

where $\zeta = z/b$, $\zeta_o \equiv (L_o - L_c)/b = 2(C - C_1 - C_2)/b$ and ζ_{exit} is defined by $V(\zeta_{exit}) = 0$. The integral S may be evaluated analytically in the interval $\zeta_o < \zeta < 0$ as well as beyond the point where the proximity potential is negligible, say $\zeta > 6$. In the intermediate range, $0 < \zeta < 6$, numerical integration has to be resorted to. If Simpson's rule is used with seven ordinates $\sqrt{V_0}$, $\sqrt{V_1}$, . . . $\sqrt{V_6}$ at $\zeta = 0,1 \ldots 6$, we find the following quite accurate approximation for S:

$$\begin{aligned} S = {} & \sqrt{V_0}\left[(-\zeta_o)^{-1} + \tfrac{1}{2}\,(V_0'/V_0)\right]^{-1} \\ & + \tfrac{1}{3}\left[(\sqrt{V_0} + \sqrt{V_6}) + 2\,(\sqrt{V_2} + \sqrt{V_4}) + 4\,(\sqrt{V_1} + \sqrt{V_3} + \sqrt{V_5})\right] \\ & - \rho_6\sqrt{V_6} + \frac{D}{\sqrt{Q}} \tan^{-1}\sqrt{V_6/Q} \quad , \end{aligned} \tag{9}$$

where $\rho_6 = (r_c/b) + 6$ is the center separation in units of b at $\zeta = 6$, $D = Z_1Z_2e^2$ and $Q = M - M_1 - M_2$ is the energy release in the disintegration. The first term in S (the contribution from the range $\zeta_o < \zeta < 0$) is obtained by making use of the following expressions for ν and $\underline{a}$ (which result from applying the smooth continuity condition on V at $z = 0$):

$$\nu = \frac{V_o'}{V_o}(-\zeta_o) \quad , \tag{10}$$

$$a = \frac{V_o}{(-\zeta_o)^\nu} \quad , \tag{11}$$

where $V_o' = \left.\frac{dV}{d\zeta}\right|_{\zeta=0} = -\frac{Z_1 Z_2 e^2 b}{r_c^2} + K\,\Phi'(0)$

$$= -\frac{Db}{r_c^2} + 0.9270\,K \quad . \tag{12}$$

To calculate $\Phi(\zeta)$ the approximation given in ref. 5 may be used:

$$\Phi(\zeta) \approx -4.41e^{-\zeta/0.7176} \qquad \text{for } \zeta \geq 1.9475 \tag{13}$$

$$\Phi(\zeta) \approx -1.7817 + 0.9270\zeta + 0.01696\zeta^2 - 0.05148\zeta^3$$

$$\text{for } 0 \leq \zeta \leq 1.9475 \quad . \tag{14}$$

Alternatively (and this is what we used) $\Phi(\zeta)$ is tabulated in ref. 4. The seven values of Φ required to evaluate eq. 9 are as follows: $\Phi(0) = -1.7817$, $\Phi(1) = -0.8594$, $\Phi(2) = -0.2689$, $\Phi(3) = -0.0674$, $\Phi(4) = -0.0167$, $\Phi(5) = -0.0042$, $\Phi(6) = -0.0010$.

3. Results

Table I shows, in column 2, the measured branching ratios (the ratios τ_α/τ_C of the lifetimes for α and ^{14}C emission) compared with the calculated ratios of the penetrability factors, G_α/G_C (column 3). The next column gives the ratios (G_α/G_C): (τ_α/τ_C). We see that the penetrability ratios are within one power of ten of the branching ratios.

Since the penetrability factors G_c (column 6) are of the order of 32-38 powers of 10, agreement to within one power of ten implies an accuracy in the penetrability integrals (involving the estimated deformation-energy barriers) of some 3%.

To test the absolute values of the lifetimes τ_α, τ_c that would be expected on the basis of this fission-like theory, we write

$$\tau_\alpha = \tau_o^\alpha \, G_\alpha \quad , \tag{15}$$

$$\tau_c = \tau_o^c \, G_c \quad , \tag{16}$$

where τ_o^α, τ_o^c are the frequency factors mentioned earlier, which ought to fall in the general range 10^{-22} - 10^{-21} sec. Column 9 shows the value of τ_o^α deduced from the experimental α-lifetime and the calculated G_α, and column 10 shows the corresponding quantity τ_o^c for ^{14}C decay. We note that in the case of α-decay the values of τ_o^α are about what one might expect, with the decay of the odd-A nucleus ^{223}Ra showing a hindrance factor of about 20 relative to its even-even neighbours. In the case of ^{14}C decay the value of τ_o^c for ^{222}Ra is in the expected range, for ^{223}Ra there seems to be present a hindrance factor of about 40 relative to ^{222}Ra and for ^{224}Ra there seems to to be an enhancement of about a factor of 6 with respect to ^{222}Ra.

4. Discussion

The reasons why the present calculations give penetrability ratios several orders of magnitude smaller than those in ref. 1 are actually two: the inclusion of the nuclear proximity interaction and the use of more realistic nuclear radii (eqs. 5,6). The nuclear proximity attraction reduces

the height and width of the barrier to be penetrated, and this is relatively more pronounced for the α-particle than for ^{14}C. This is because the proximity attraction is proportional to the reduced radius $C_1C_2(C_2 + C_2)$, which scales (approximately) as the cube root $A_2^{1/3}$ of the mass number of the small fragment, whereas the Coulomb repulsion scales approximately as the atomic number Z_2, roughly proportional to A_2. The ratio of the nuclear to the Coulomb potential, proportional to $A_2^{-2/3}$, increases with decreasing A_2.

The other reason for the enhanced emission of α-particles in the present calculations is the use of realistic nuclear radii. First of all, one must realize that the radius relevant for locating the surfaces of interacting nuclei is the central radius C or the approximately equivalent half-density radius $C_{1/2}$ (where the nuclear density has dropped to half its central value) and not the effective sharp radius R, which is the quantity approximately proportional to $A^{1/3}$. (See ref. 4.). Now the central radius C (or $C_{1/2}$) would not be proportional to $A^{1/3}$ even if nuclei were incompressible and R were exactly proportional to $A^{1/3}$. Instead, C is related (approximately) to R by eq. 5. (This equation is a consequence of a simple piece of geometry, namely the greater weight carried by the tail of a diffuse density distribution, due to the geometrical r^2-weighting of radial volume integrals.) The result is that C falls below R by an amount that increases with decreasing size of the nucleus. (See ref. 4.) For the light nuclei in question, the difference can be quite substantial. Thus, according to eqs. 5,6, the effective sharp radius R is 1.776 fm for an α-particle and 2.657 fm for ^{14}C, whereas the central radii C are 1.213 fm and 2.281 fm, respectively. (These values are close to the measured half-density radii for ^4He and ^{12}C, ref. 6.) The corresponding values of $R/A^{1/3}$ are 1.119 fm

for the α-particle and 1.102 for ^{14}C, in conformity with the approximate incompressibility of nuclei. On the other hand, if one tried (incorrectly) to reproduce the central radii by a formula of the type $r_0 A^{1/3}$, one would have to use $r_0 = 0.764$ fm for A = 4 and $r_0 = 0.946$ fm for A = 14--values that would be considered quite unconventional, and significantly smaller for the α-particle than for ^{14}C.

Our semi-empirical formulae for the central radii C, although fairly realistic, do not reproduce the measured half-density radii exactly. For example, the half-density radius of ^{4}He is given in ref. 6 as 1.33-1.34 fm. Using $C_2 = 1.335$ fm (instead of 1.213 fm) would give, for the case of ^{222}Ra decay, a penetrability factor $G_\alpha = 4.946 \times 10^{22}$. This represents an enhancement of α-emission by a factor 5.83. Such enhancements would lead to calculated penetrability ratios of 2.88×10^{-10}, 1.18×10^{-9} and 1.05×10^{-11} in the case of ^{222}Ra, ^{223}Ra and ^{224}Ra, which numbers differ from the measured branching ratios by factors of 0.78, 1.93 and 0.24 (instead of the 4.5, 11.3 and 1.43 in Table I).

A better estimate of the radius of ^{14}C might lead to similar changes in the calculated penetrability ratios. In any case, at the level of agreement to within a factor of 10 or so, (corresponding to a few percent accuracy in the penetrability integrals) the measured branching ratios for the three Ra isotopes can be accounted for in terms of a fission-like treatment of the disintegrations. The absolute values of the lifetimes indicate the presence of hindrance factors for the odd-A nucleus ^{223}Ra not accounted for by the present treatment. (Such odd-nucleon hindrance factors are a familiar feature of both α- and fission-decay systematics). The unexplained enhancement of the ^{14}C decay of ^{224}Ra with respect to ^{222}Ra, implied by our estimates of

τ_o^c, underlines the need for caution in making more than qualitative predictions as regards the lifetimes (and branching ratios) for other exotic decays. Also, when the emission of heavier and heavier fragments comes into question, one should bear in mind the serious limitation of the present estimates, based as they are on a deformation energy which combines the Coulomb and proximity forces of spherical fragments. In the limit of fission into comparable fragments it is, of course, well known that such a treatment would give meaningless results: the actual deformation energies and fission barriers of heavy nuclei bear no resemblance whatever to what a calculation based on spherical fragments would suggest. Thus, for fragments heavier than ^{14}C, it will at some stage be essential to consider in quantitative detail the appearance of the potential-energy barrier in the regime where the two-sphere approximation is not adequate (i.e. for $L \lesssim L_c$). Fig. 2(b) illustrates the case of $^{232}U \rightarrow {}^{208}Pb + {}^{24}Ne$, where this problem might already be a serious one. About 23% of the penetrability integral comes in this case from the region $L_o < L < L_c$, where we use an arbitrary and uncertain interpolation. Adding to this the expected modifications in the barrier caused by fragment deformations and neck formation, one might well expect that a fair fraction of the potential-energy barrier could be significantly changed by a more adequate treatment. Without being able to estimate quantitatively at this stage how soon beyond ^{14}C these effects will come in and how drastic they will be, it seems fairly safe to conjecture that, by and large, the two-sphere approximation, used in the present work, will tend to overestimate the decay lifetimes of the heavier fragments because the inclusion of a richer variety of deformation variables would allow the disintegrating system to seek out a more favorable path in configuration space in the process of barrier

penetration. One may even speculate that the enhancement of ^{14}C emission in the case of ^{224}Ra (compared to ^{222}Ra) could be a precursor of such fragment-deformation effects, the daughter nucleus ^{210}Pb being somewhat more deformable than the doubly magic nucleus ^{208}Pb.

With all these reservations in mind we prepared a survey of nominal penetrability factors for a large number of potentially interesting disintegrations, using the equations described in this paper. This included all disintegrations ending in the isotopes of lead from ^{206}Pb to ^{214}Pb, the emitted fragments being all the isotopes of Be, B, C, O, Ne, Mg, Si and S for which the atomic masses are listed in Wapstra et al.'s 1984 compilation, ref. 7. (The parent nuclei were thus various isotopes of Rn, Fr, Ra, Th, U, Pu, Cm and Cf. Some of these have dominant β-decay branches and would not be relevant candidates for the study of heavy-particle radioactivity.) In most cases the penetrability ratios G_α/G_X (X stands for the emitted fragment) were many orders of magnitude less favourable than in the three cases listed in Table I, but there were notable exceptions. In Table II we have listed some particulars of all disintegrations for which G_α/G_X was calculated to be greater than 10^{-12}. The list includes the decay of three additional isotopes of Ra by ^{14}C emission, four isotopes of Th decaying by ^{22}O emission and four isotopes of U decaying by the emission of ^{24}Ne, ^{25}Ne or ^{26}Ne. Column 3 in Table II shows the calculated penetrability ratios normalized to the corresponding ratios for disintegrations involving a ^{14}C fragment and the same daughter isotope of Pb.

In Table III we give the results of a similar search for disintegrations with calculated penetrability ratios $>10^{-12}$, but with isotopes of Hg, Tl and Bi as end products. We also considered decays involving fragments with an odd atomic number (ending up in either Tl, Pb or Bi isotopes), but there was not a single candidate of this type with a penetrability ratio $>10^{-12}$.

Other decays than those shown in Tables II and III might eventually become observable with improvements in the detection techniques. One should also keep in mind the possibility, mentioned earlier, that for the heavier fragments the ratios G_α/G_χ in Tables II and III might be underestimates--perhaps by large factors. The observation of even one of the cases involving O or Ne isotopes would be extremely valuable in providing information on the degree of improvement in the branching ratios to be expected from the anticipated effect of fragment deformations during barrier penetration.

Acknowledgements

We would like to thank S. Gales, A Ghiorso, M. Nitschke, P. B. Price and S. Yashita for valuable discussions. One of us (S.Y-J.) would like to acknowledge the hospitality of the Theory Group of the Lawrence Berkeley Laboratory's Nuclear Science Division.

This work was supported by the Director, Office of Energy Research, Division of Nuclear Physics of the Office of High Energy and Nuclear Physics of the U.S. Department of Energy under Contract DE-AC03-76SF00098.

References

1. H. J. Rose and G. A. Jones, Nature 307 (1984) 245.

2. S. Gales, E. Hourani, M. Hussonnois, J. P. Schapira, L. Stab and M. Vergnes, Phys. Rev. Lett. 53 (1984) 759.

3. P. B. Price, J. D. Stevenson, S. W. Barwick and H. L. Ravn, "Discovery of Radioactive Decay of ^{222}Ra and ^{224}Ra by ^{14}C Emission," 1984 preprint, submitted to Phys. Rev. Letters.

4. J. Blocki, J. Randrup, W. J. Swiatecki and C. F. Tsang, Ann. Phys. 105 (1977) 427.

5. J. Blocki and W. J. Swiatecki, Ann. Phys. 132 (1981) 53.

6. R. Hofstadter and H. R. Collard, "Nuclear Radii," Landolt-Bornstein Numerical Data and Functional Relationships, 2, Springer-Verlag, 1967.

7. R. Firestone, private communication, 1984.

8. D. N. Poenaru, M. Ivascu, A. Sandulescu and W. Greiner, J. Phys. G: Nucl. Phys. 10 (1984) L183 and references therein.

Figure Captions

1. The deformation-energy barrier V(L) for the emisson of an α-particle, (a), or a ^{14}C nucleus, (b), from ^{222}Ra. The dashed curves are the integrands in the penetrability integral. The total extension of the configuration is L and the distance between the near surfaces of the fragments is z. Most of the barrier corresponds to separated fragments (the region to the right of the vertical line at z = 0).

2. Same as Fig. 1, but for the decay of ^{232}U.

TABLE I

Alpha particle and ^{14}C emissions from

three isotopes of Ra

Parent Nucleus	Experimental τ_α/τ_C	Calculated G_α/G_C	$\frac{G_\alpha}{G_C} : \frac{\tau_\alpha}{\tau_C}$	Calculated G_α	Calculated G_C
^{222}Ra	$(3.7 \pm 0.5) \times 10^{-10}$	1.678×10^{-9}	4.5	2.884×10^{23}	1.718×10^{32}
^{223}Ra	$(6.1 \pm 0.8) \times 10^{-10}$	6.895×10^{-9}	11.3	4.717×10^{26}	6.842×10^{34}
^{224}Ra	$(4.3 \pm 1.1) \times 10^{-11}$	6.150×10^{-11}	1.43	4.378×10^{27}	7.119×10^{37}

	Experimental τ_α(sec)	Experimental τ_C(sec)	Deduced τ_o^α (sec)	Deduced τ_o^C (sec)
^{222}Ra	38	1.03×10^{11}	1.32×10^{-22}	5.98×10^{-22}
^{223}Ra	0.985×10^{6}	1.62×10^{15}	2.09×10^{-21}	2.36×10^{-20}
^{224}Ra	0.311×10^{6}	7.23×10^{15}	0.71×10^{-22}	1.02×10^{-22}

TABLE II

Some properties of distintegrations to isotopes of Pb

with calculated penetrability ratios $>10^{-12}$

Disintegration	G_α/G_X	$\frac{G_\alpha/G_X}{G_\alpha/G_C}$	G_X	G_α
$^{221}Ra \rightarrow {}^{207}Pb + {}^{14}C$	8.181×10^{-12}	1	5.307×10^{33}	4.342×10^{22}
$^{222}Ra \rightarrow {}^{208}Pb + {}^{14}C$	1.678×10^{-9}	1	1.718×10^{32}	2.884×10^{23}
$^{223}Ra \rightarrow {}^{209}Pb + {}^{14}C$	6.895×10^{-9}	1	6.842×10^{34}	4.717×10^{26}
$^{224}Ra \rightarrow {}^{210}Pb + {}^{14}C$	6.150×10^{-11}	1	7.119×10^{37}	4.378×10^{27}
$^{225}Ra \rightarrow {}^{211}Pb + {}^{14}C$	6.992×10^{-10}	1	2.781×10^{40}	1.944×10^{31}
$^{226}Ra \rightarrow {}^{212}Pb + {}^{14}C$	3.081×10^{-11}	1	4.229×10^{43}	1.303×10^{33}
$^{230}Th \rightarrow {}^{208}Pb + {}^{22}O$	3.520×10^{-12}	0.0021	2.616×10^{46}	9.209×10^{34}
$^{231}Th \rightarrow {}^{209}Pb + {}^{22}O$	1.263×10^{-10}	0.0183	1.744×10^{49}	2.203×10^{39}
$^{232}Th \rightarrow {}^{210}Pb + {}^{22}O$	1.332×10^{-12}	0.0217	2.327×10^{52}	3.100×10^{40}
$^{233}Th \rightarrow {}^{211}Pb + {}^{22}O$	1.185×10^{-12}	0.0017	7.488×10^{54}	8.873×10^{42}
$^{231}U \rightarrow {}^{207}Pb + {}^{24}Ne$	3.954×10^{-12}	0.4833	2.877×10^{42}	1.138×10^{31}
$^{232}U \rightarrow {}^{208}Pb + {}^{24}Ne$	4.872×10^{-11}	0.0290	1.485×10^{42}	7.235×10^{31}
$^{233}U \rightarrow {}^{209}Pb + {}^{24}Ne$	3.747×10^{-11}	0.0054	3.748×10^{45}	1.404×10^{35}
$^{233}U \rightarrow {}^{208}Pb + {}^{25}Ne$	2.556×10^{-10}	0.1523	5.493×10^{44}	1.404×10^{35}
$^{234}U \rightarrow {}^{208}Pb + {}^{26}Ne$	1.565×10^{-12}	0.0009	1.981×10^{47}	3.100×10^{35}

TABLE III

Some properties of distintegrations to isotopes of Hg, Tl and Bi, with calculated penetrability ratios $>10^{-12}$

Disintegration	G_α/G_X	G_X	G_α
$^{231}Th \rightarrow {}^{207}Hg + {}^{24}Ne$	2.466×10^{-12}	8.931×10^{50}	2.203×10^{39}
$^{231}Th \rightarrow {}^{206}Hg + {}^{25}Ne$	2.278×10^{-10}	9.668×10^{48}	2.203×10^{39}
$^{232}Th \rightarrow {}^{206}Hg + {}^{26}Ne$	3.666×10^{-11}	8.455×10^{50}	3.100×10^{40}
$^{233}Th \rightarrow {}^{207}Hg + {}^{26}Ne$	8.687×10^{-12}	1.021×10^{54}	8.873×10^{42}
$^{221}Fr \rightarrow {}^{207}Tl + {}^{14}C$	7.988×10^{-12}	1.089×10^{35}	8.698×10^{23}
$^{222}Fr \rightarrow {}^{208}Tl + {}^{14}C$	1.283×10^{-11}	5.373×10^{37}	6.894×10^{26}
$^{223}Fr \rightarrow {}^{209}Tl + {}^{14}C$	4.481×10^{-12}	2.485×10^{40}	1.114×10^{29}
$^{224}Fr \rightarrow {}^{210}Tl + {}^{14}C$	7.814×10^{-12}	2.259×10^{43}	1.765×10^{32}
$^{229}Ac \rightarrow {}^{207}Tl + {}^{22}O$	7.315×10^{-11}	7.455×10^{46}	5.454×10^{36}
$^{230}Ac \rightarrow {}^{208}Tl + {}^{22}O$	3.293×10^{-11}	7.453×10^{49}	2.454×10^{39}
$^{231}Ac \rightarrow {}^{209}Tl + {}^{22}O$	1.926×10^{-11}	2.011×10^{52}	3.873×10^{41}
$^{232}Ac \rightarrow {}^{210}Tl + {}^{22}O$	4.915×10^{-12}	1.252×10^{55}	6.156×10^{43}
$^{231}Pa \rightarrow {}^{207}Tl + {}^{24}Ne$	9.448×10^{-12}	9.798×10^{43}	9.258×10^{32}
$^{232}Pa \rightarrow {}^{208}Tl + {}^{24}Ne$	2.210×10^{-11}	2.620×10^{47}	5.792×10^{36}
$^{233}Pa \rightarrow {}^{209}Tl + {}^{24}Ne$	2.327×10^{-12}	3.329×10^{50}	7.746×10^{38}
$^{232}Pa \rightarrow {}^{207}Tl + {}^{25}Ne$	2.701×10^{-10}	2.144×10^{46}	5.792×10^{36}
$^{234}Pa \rightarrow {}^{209}Tl + {}^{25}Ne$	1.232×10^{-12}	2.637×10^{52}	3.247×10^{40}
$^{233}Pa \rightarrow {}^{207}Tl + {}^{26}Ne$	4.017×10^{-10}	1.929×10^{48}	7.746×10^{38}
$^{234}Pa \rightarrow {}^{208}Tl + {}^{26}Ne$	1.775×10^{-11}	1.829×10^{51}	3.247×10^{40}
$^{235}Pa \rightarrow {}^{209}Tl + {}^{26}Ne$	2.227×10^{-12}	4.925×10^{53}	1.097×10^{42}
$^{235}Np \rightarrow {}^{207}Tl + {}^{28}Mg$	1.101×10^{-12}	5.557×10^{45}	6.116×10^{33}
$^{223}Ac \rightarrow {}^{209}Bi + {}^{14}C$	1.564×10^{-10}	1.954×10^{33}	3.056×10^{23}
$^{224}Ac \rightarrow {}^{210}Bi + {}^{14}C$	7.249×10^{-11}	4.467×10^{35}	3.238×10^{25}
$^{225}Ac \rightarrow {}^{211}Bi + {}^{14}C$	1.629×10^{-12}	1.546×10^{39}	2.519×10^{27}

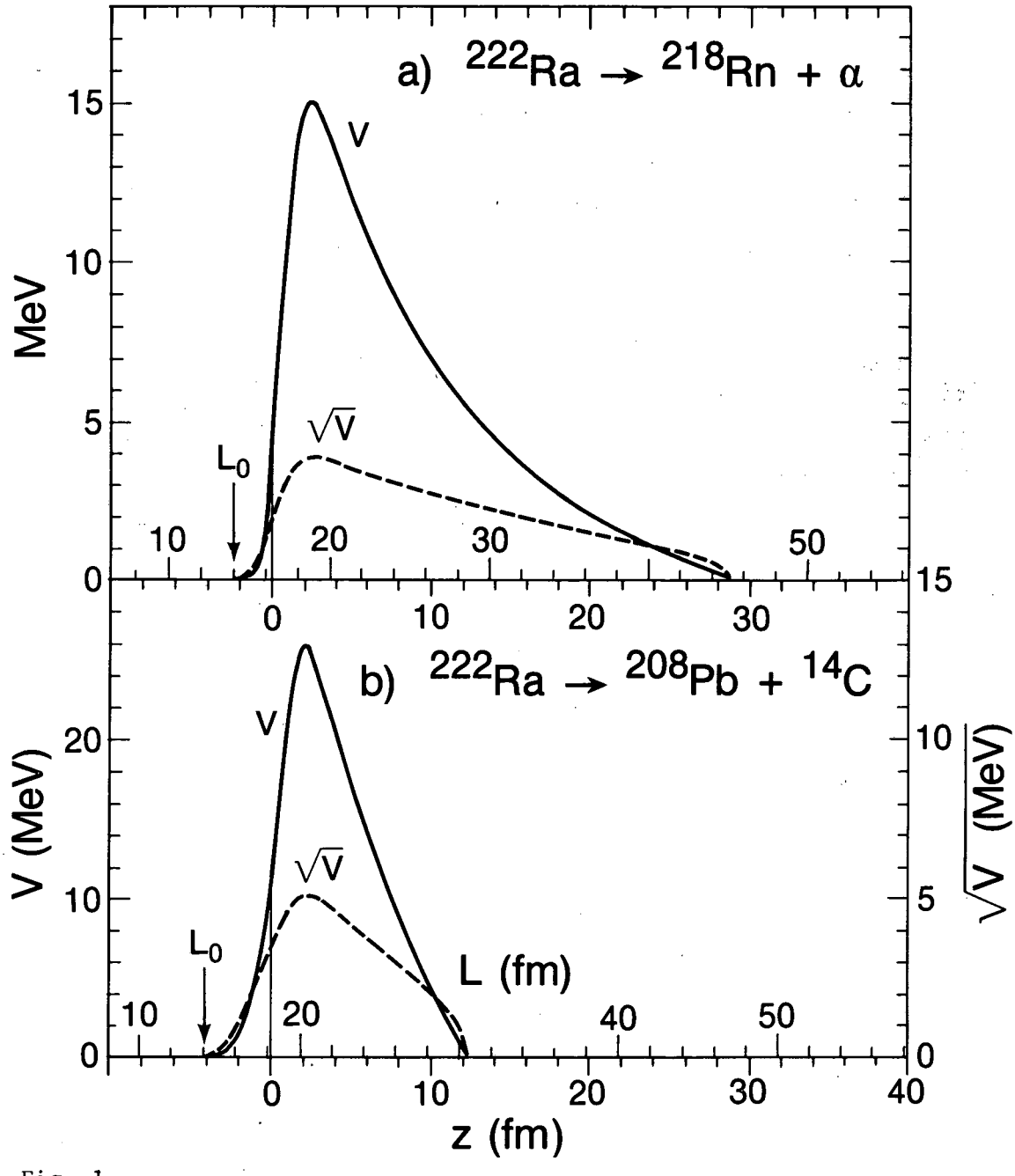

Fig. 1

XBL 848-8842

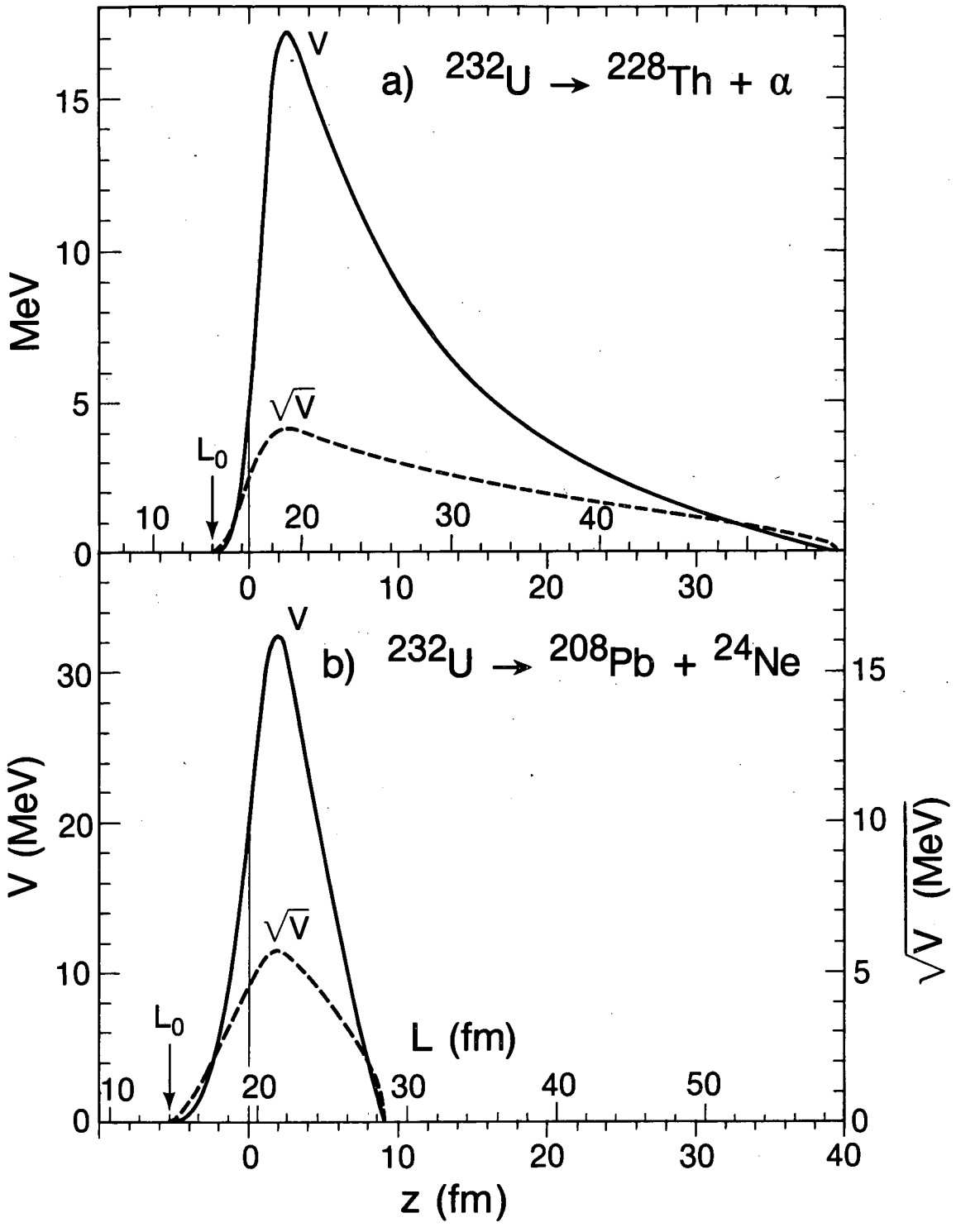

Fig. 2

XBL 848-8841

This report was done with support from the Department of Energy. Any conclusions or opinions expressed in this report represent solely those of the author(s) and not necessarily those of The Regents of the University of California, the Lawrence Berkeley Laboratory or the Department of Energy.

Reference to a company or product name does not imply approval or recommendation of the product by the University of California or the U.S. Department of Energy to the exclusion of others that may be suitable.

TECHNICAL INFORMATION DEPARTMENT
LAWRENCE BERKELEY LABORATORY
UNIVERSITY OF CALIFORNIA
BERKELEY, CALIFORNIA 94720